N85-22493

SURFACE INTERACTIONS AND HIGH-VOLTAGE CURRENT COLLECTION*

M. J. Mandell and I. Katz
S-CUBED
La Jolla, California 92038

Spacecraft of the future will be larger and have higher power requirements than any flown to date. For several reasons, it is desirable to operate a high-power system at high voltage. While the optimal voltages for many future missions are in the range 500-5000 volts, the highest voltage yet flown is ∿100 volts. (For a proposed solar power satellite, voltages as high as 40 kV have been mentioned.)

S-CUBED, under contract to NASA/Lewis Research Center, is developing the NASCAP/LEO (ref. 1) code to embody the phenomenology needed to model the environmental interactions of high voltage spacecraft. In this paper we will discuss some aspects of the interaction between a high voltage spacecraft and its plasma environment. We will also describe the treatment of the surface conductivity associated with emitted electrons. Finally, we will excerpt some simulations by NASCAP/LEO of ground-based high-voltage interaction experiments.

PLASMA INTERACTIONS

Table 1 shows two representative low-orbit environments compared with a typical geosynchronous plasma. The low orbit plasma is far colder and denser, resulting in a short (∿1 cm) Debye length. The short Debye length is deceptive, however, as a high voltage spacecraft will expel plasma from its vicinity. A better estimate (refs. 2-4) of the collection distance is provided by the Child-Langmuir length

$$D_{CL} = (4\varepsilon_o/9)^{1/2} (4\pi/e\theta)^{1/4} n^{-1/2} |\phi|^{3/4}$$

where θ is the plasma temperature (eV), ϕ the surface potential, and n the plasma density. This expression is derived by equating the plasma thermal electron current to the current collected by a space-charge-limited planar diode operating at the surface voltage, and solving for the plate separation. As shown in Table 1, this distance can easily be many meters for a kilovolt bias. It follows that the "sheath surface", which divides the high voltage region from relatively unperturbed plasma, will not be within a few Debye lengths of the

*This work supported by NASA/Lewis Research Center, Cleveland, OH, under Contract NAS3-23058.

spacecraft surface (thin sheath approximation), nor will it be far distant from the spacecraft (orbit-limited approximation), but it will be in an intermediate regime such that the full spacecraft geometry must be taken into account.

TABLE 1.-TYPICAL PLASMA PARAMETERS FOR LEO AND GEO

	GEO (Typical)	LEO (Low Density)	LEO (High Density)
Density (m^{-3})	10^6	10^{10}	10^{12}
Temperature (eV)	10^3	0.3	0.1
Debye Length (m)	235	0.04	0.002
Electron Thermal Current (A/m^2)	10^6	10^{-4}	10^{-2}
Ram Ion Current (A/m^2)	5×10^{-10}	10^{-5}	10^{-3}
Ion (O^+) Mach Number	0.04	6.0	10.0
Current Collection D_{CL}	Orbit Limited	Space-Charge Limited 22 m at 1 kV	Space-Charge Limited 3 m at 1 kV

Currents to a large spacecraft are indicated schematically in figure 1. The primary current to the negative surfaces consists of ram ions, while the positive surfaces collect thermal electrons. As the ram ion current is only about one-tenth the electron thermal current, the spacecraft will float about 90 percent negative. However, for high bias the ion current will be enhanced by ion-generated secondary electrons. An additional source current to negative surfaces is charge blowoff from arc discharges. As discussed elsewhere in this volume (refs. 5-7), discharges on solar arrays have been observed for negative biases as low as ∿250 V.

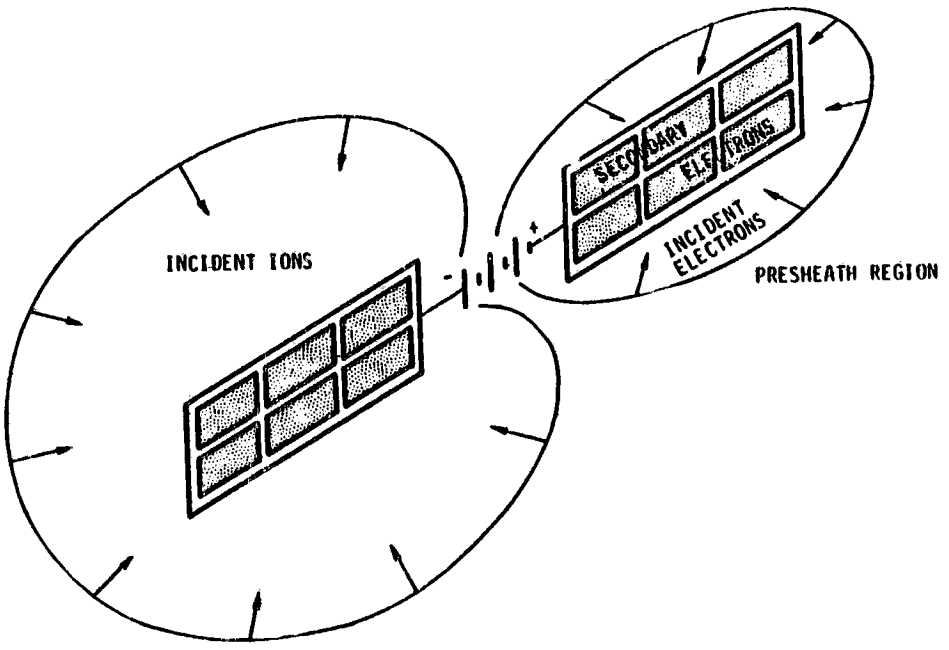

Figure 1. A high-voltage spacecraft collects ions and electrons from a plasma.

Positive surfaces attract plasma electrons, and the resultant secondary electrons form a conductive layer over the surface, as discussed below. Due to smoothing of voltage gradients provided by this effect, positively biased array surfaces are much less likely to arc than negatively biased surfaces.

The plasma currents collected by array surfaces constitute a parasitic current through the array. The effects of this parasitic current on array operation were discussed at the 1978 Spacecraft Charging Technology Conference by Domitz and Kolecki (ref. 8). As shown in figure 2a, solar cells maintain a nearly constant voltage up to a maximum current. When this current is exceeded the voltage drops sharply to zero. Clearly, it is advantageous to operate as closely as possible to the solar cell's power peak (figure 2b). Figure 3a illustrates that plasma current is collected in a distributed fashion over the array. The parasitic current at any point of the array is the integral of the plasma current density. Figure 3b shows a case in which a relatively small parasitic current, when added to the load current, shorts out the central portion of the array.

THE NASCAP/LEO CODE

NASCAP/LEO is being developed to predict self-consistently surface potentials, collected currents, and spatial electric fields for high voltage spacecraft in dense plasmas. While much of the code's algorithmic structure is adapted from the widely used NASCAP code (ref. 9), NASCAP/LEO also contains several noteworthy features necessary for modeling the intended physical regimes.

NASCAP/LEO has NASCAP-like object definition routines. Like NASCAP, the object is contained in a primary grid (figure 4), which may be surrounded by one or more outer grids with successively doubled mesh spacing. Enhancements include the ability to put mirror planes coincident with one or more of the inner grid boundary planes, and to include subdivided regions in the primary grid in order to resolve small but important object features.

Space charge, which is typically ignored in NASCAP, is treated by NASCAP/LEO as a local, nonlinear function of potential. Presently the function is taken to be

$$\rho = -(\varepsilon_o \phi/\lambda_D)^2 \left[1 + \sqrt{4\pi}\ (\phi/\theta)^{3/2}\right]^{-1}$$

A particularly important enhancement in NASCAP/LEO is the ability to apply either potential or normal-electric-field boundary conditions to each surface cell. The field condition is used for cells whose potential is governed by emission of low energy electrons (see below).

To calculate plasma currents, NASCAP/LEO defines the sheath surface as a specified equipotential, and tracks representative particles inward. The current represented by each particle is determined taking into account ram effects as well as the local plasma density and temperature. Care is taken not to generate sheath particles in regions from which plasma is excluded by high fields or by nearby object surfaces. Thus NASCAP/LEO determines the ion and electron currents to an

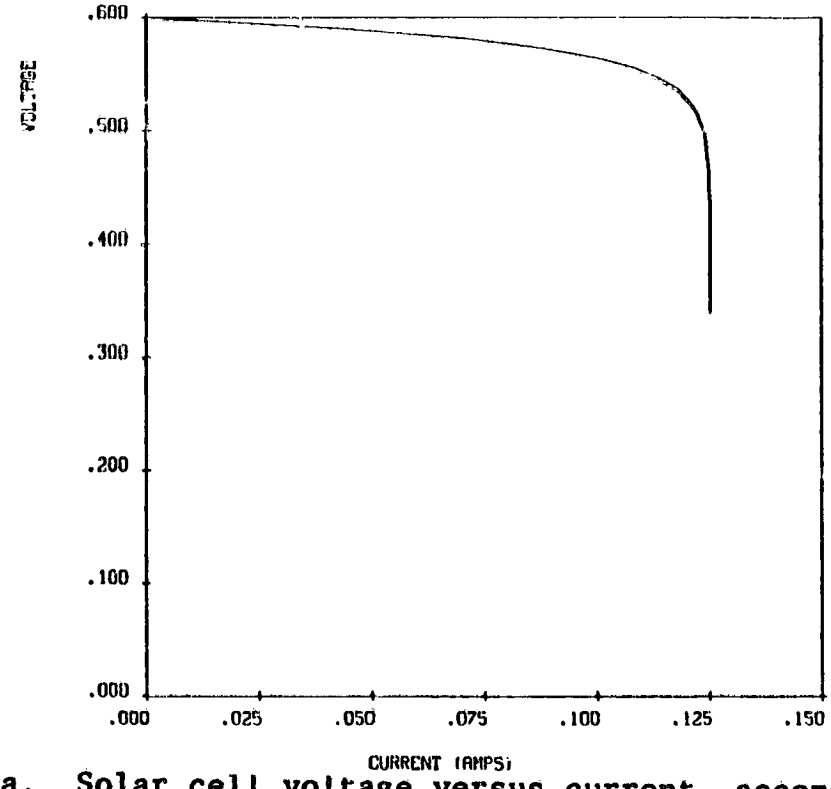

Figure 2a. Solar cell voltage versus current, according to Domitz and Kolecki (ref. 8).

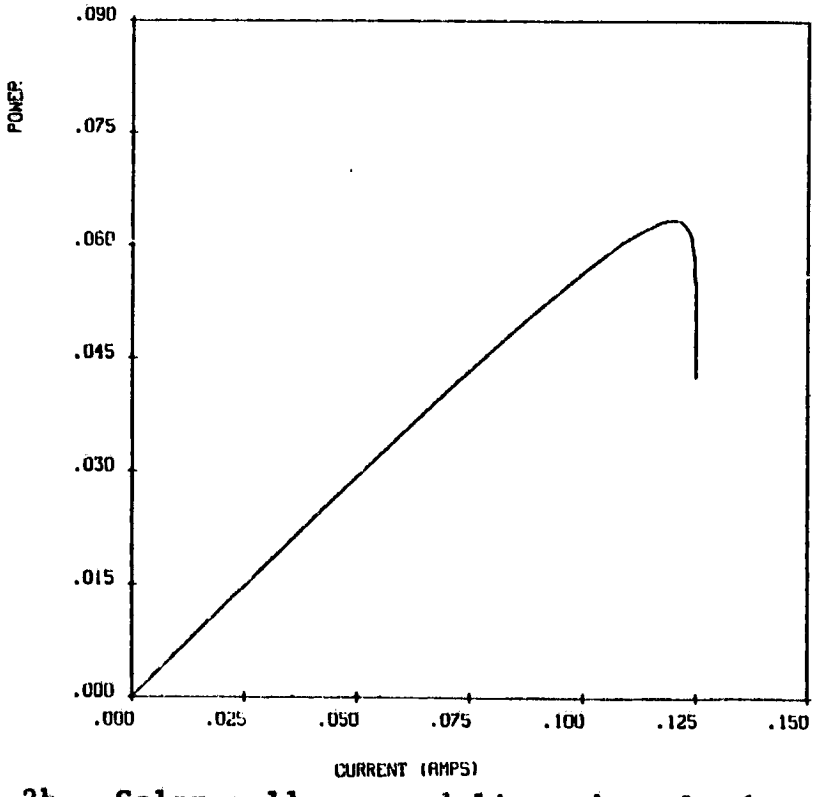

Figure 2b. Solar cell power delivered to load versus current, according to Domitz and Kolecki (ref. 8).

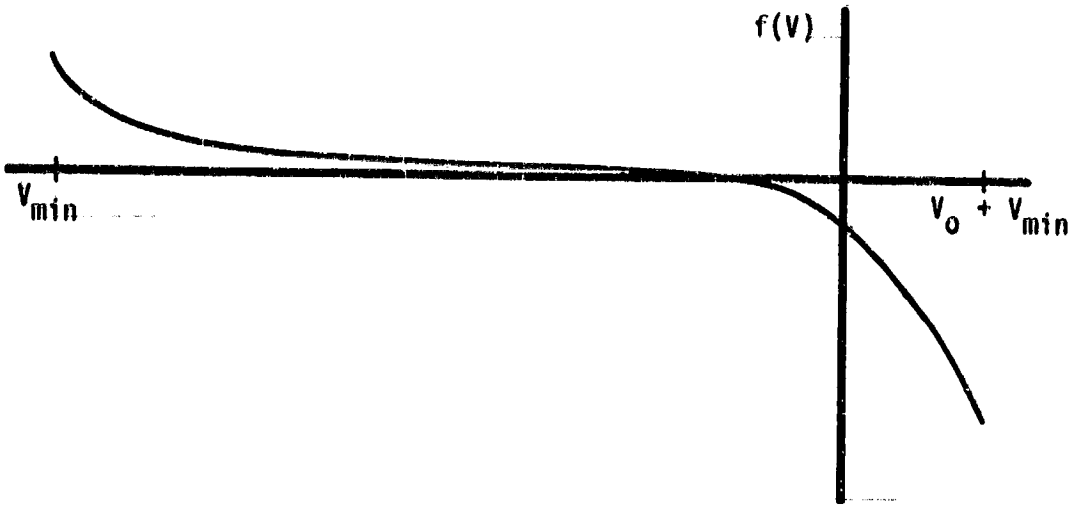

Figure 3a. Plasma current density, f(V), to a solar array (schematic).

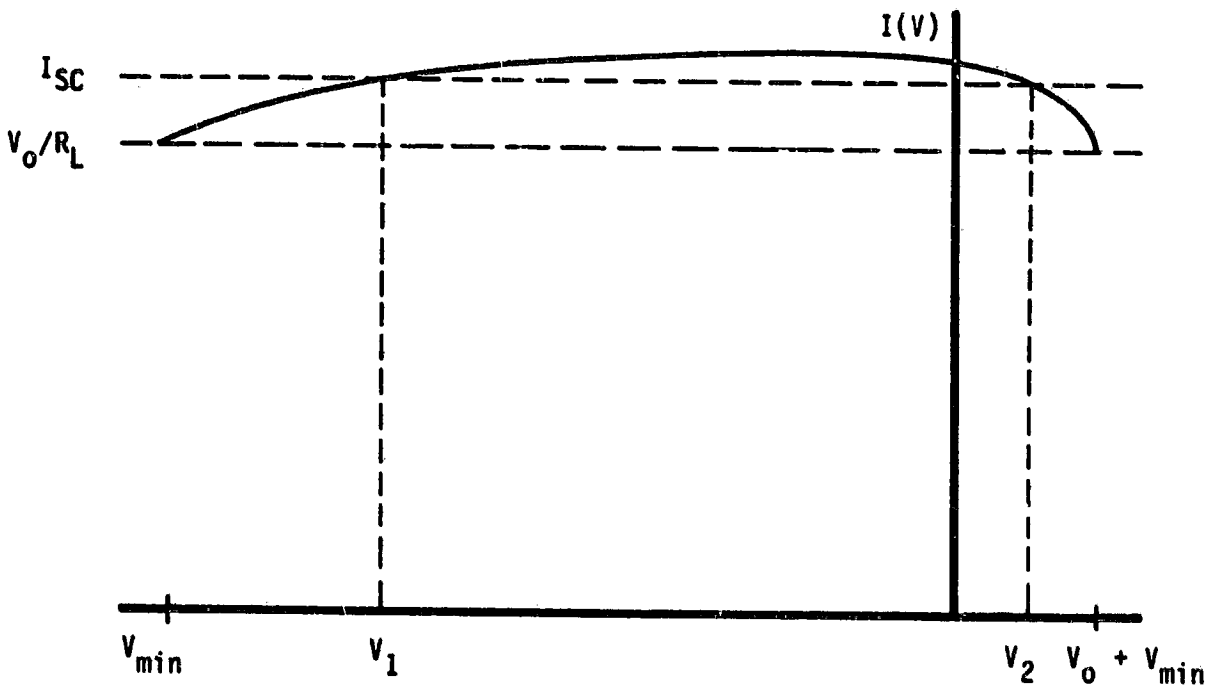

Figure 3b. Total array current as a function of voltage (solid line; schematic), consists of load current, V_o/R_L, plus parasitic current. For this case, a substantial part of the array will be shorted out.

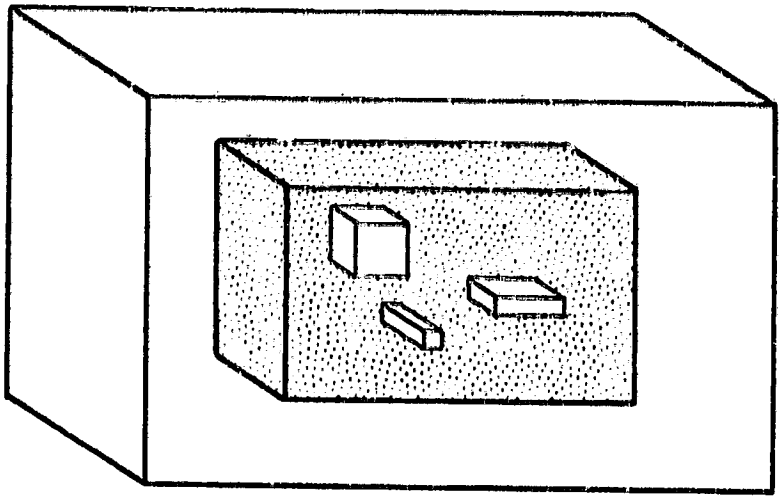

Figure 4. NASCAP/LEO grid structure, showing primary grid (shaded), outer grid, and locally subdivided regions.

object, as well as the distribution of current over the object.

ELECTRIC FIELD BOUNDARY CONDITIONS

For electron attracting insulating surfaces dominated by secondary electron emission, NASCAP/LEO sets an electric field boundary condition such that the incident electron current is balanced by a net outflow of secondaries to neighboring surfaces. The derivation of electron hopping conductivity has been presented elsewhere (refs. 10-11), but we repeat it here for completeness, then proceed to derive the electric field boundary condition.

Assume a surface has an electron-attracting (positive) surface-normal component of electric field, $E_\perp$, and emits a low energy electron current $-J_e(A/m^2)$. These electrons travel in parabolic orbits, with "flight time", τ, given by

$$\tau = 2\,[2m\langle\varepsilon\rangle/e\,E_\perp^2]^{1/2}$$

where m is the electron mass and $\langle\varepsilon\rangle$ is the (appropriately averaged) electron energy. These electrons form a charge density (coul/m^2) given by $-J_e\tau$. This surface charge layer will be accelerated by any transverse electric field, $E_\parallel$, to a mean velocity of $-e\,E_\parallel\tau/2m$, and thus constitutes a surface current, K (A/m) given by

$$K = (-J_e\tau^2/2)(-e\,E_\parallel/m) = 4\,J_e\,E_\parallel\langle\varepsilon\rangle/E_\perp^2 = \sigma_\parallel E_\parallel$$

The last relation defines the transverse conductivity, $\sigma_\parallel$ (ohms^{-1}).

To derive the electric field boundary condition, we further assume that the emitted current is proportional to the incident current, J_{in}:

$$J_e = -Y\,J_{in}$$

Current balance requires that

$$J_{in} = \nabla\cdot(\sigma_{\parallel} E_{\parallel}) \ .$$

Since the previous derivation assumed uniform fields, it is no further approximation to remove $\sigma_{\parallel}$ from the divergence, giving

$$J_{in} = [4(-Y J_{in}) <\varepsilon>/E_{\perp}^2] \ (\nabla\cdot E_{\parallel}) \ .$$

The incident current cancels from the above equation, which may then be solved for the desired condition:

$$E_{\perp} = [-4 \ Y<\varepsilon> \ (\nabla\cdot E_{\parallel})]^{1/2} \ .$$

ILLUSTRATIVE CALCULATIONS

To illustrate the type of information obtainable from the NASCAP/LEO code we present results from three previously published simulations of laboratory experiments. For more details we refer the reader to the original publications (refs. 1, 2, 12).

Early NASCAP/LEO calculations were restricted to potentials about, and current collection by, surfaces of known potential. McCoy and Konradi (ref. 3) reported at the 1978 Spacecraft Charging Technology Conference experiments on a biasable metal strip, about 10 meters long, mounted on insulating plastic. Figure 5 shows sheath trajectories for cases in which the metal strip was linearly biased. The four cases are 0-600 V, 0-1200 V, 0-2400 V, and 0-4800 V. The shape of the sheath, as indicated by the plotted trajectories, is in agreement with observations by low-light-level television. Also, the calculated and measured currents are in good agreement.

NASCAP/LEO was later improved to predict the spread of high voltages onto insulating surfaces. N. John Stevens (ref. 13) reported experiments in which a 3.5 cm diameter biased metal disk (figure 6) was surrounded by either grounded metal or by kapton, and the collected current was measured. For the "plain disk" case (figure 7) agreement was excellent. The Disk-on-Kapton case (figure 8) is far more difficult, as the kapton enhances collected current at high bias voltage, and suppresses it at low voltage. While the simulation results were in fair agreement at high bias, both for collected current and insulator surface voltage (figure 9) they did not predict the low voltage current suppression. This was because the charging algorithm at the time was unable to predict negative charging of the kapton surfaces.

A similar experiment was reported by S. Gabriel et al. (ref. 15), who used an emissive probe to measure the electrostatic potential in the plasma over a biased "pinhole". The computer model (figure 10) made use of the NASCAP/LEO subdivision capability to get good spatial resolution in the neighborhood of the pinhole. For negative bias (figure 11) agreement was excellent. Fairly good agreement was also obtained for positive bias (figure 12), although the experiment showed more distinction between two different plasmas than the calculations predicted. Good agreement was achieved as well for the collected currents. This latter calculation showed the utility of the

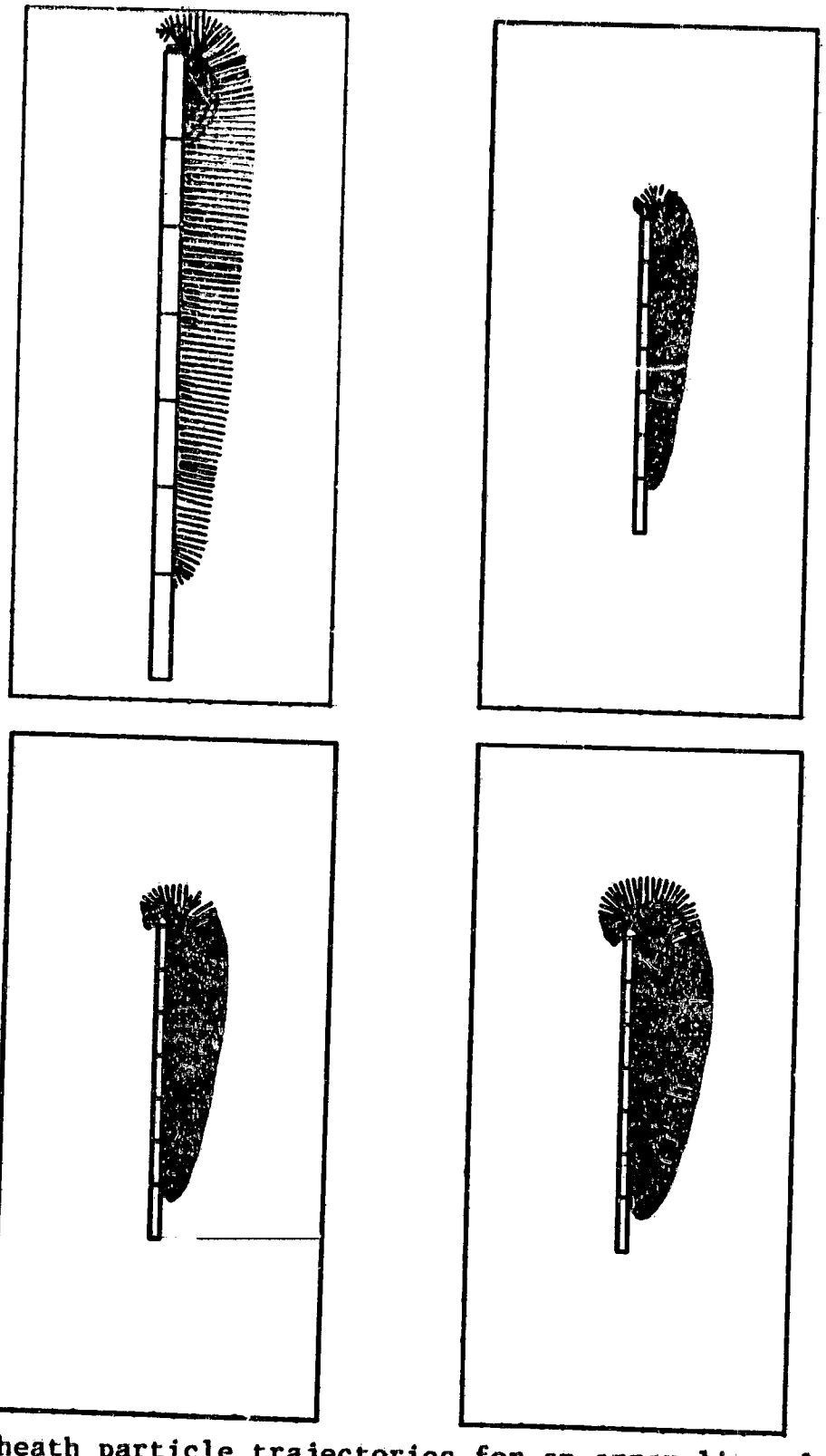

Figure 5. Sheath particle trajectories for an array linearly biased 0-600 volts (upper left; twice scale); 0-1200 volts (upper right); 0-2400 volts (lower left); and 0-4800 volts (lower right).

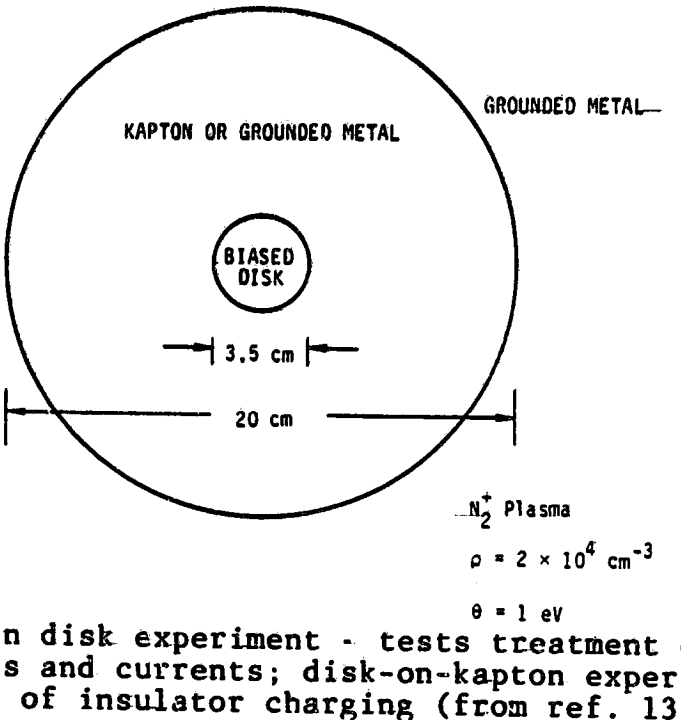

Figure 6. Plain disk experiment - tests treatment of external potentials and currents; disk-on-kapton experiment - tests treatment of insulator charging (from ref. 13).

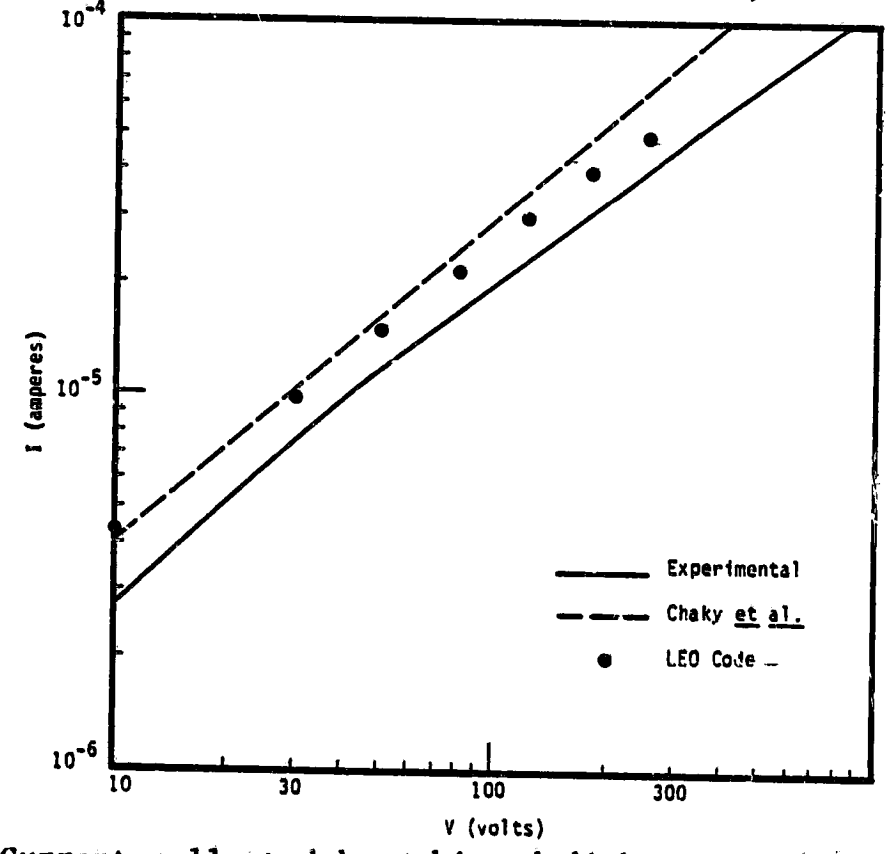

Figure 7. Current collected by a biased disk surrounded by grounded metal. The dashed curve is a prediction by a two-dimensional particle-in-cell code (ref. 14).

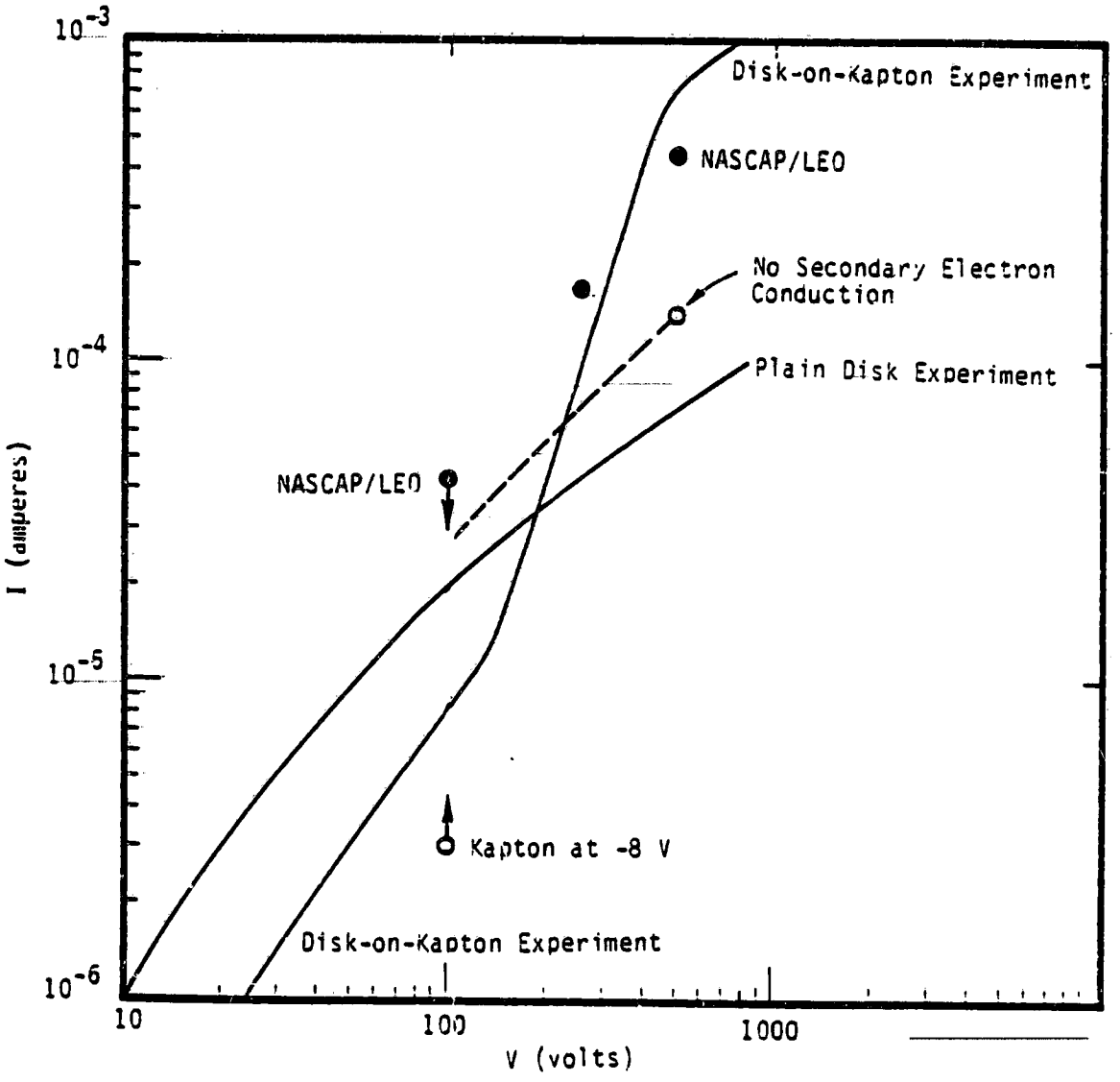

Figure 8. Current collected by a biased disk surrounded by kapton. For high bias, NASCAP/LEO correctly predicts current enhancement (relative to the plain disk). For low bias current is suppressed due to accumulation of negative charge on the kapton. At the time of the calculation the NASCAP/LEO charging algorithm did not predict negative floating potential for insulators.

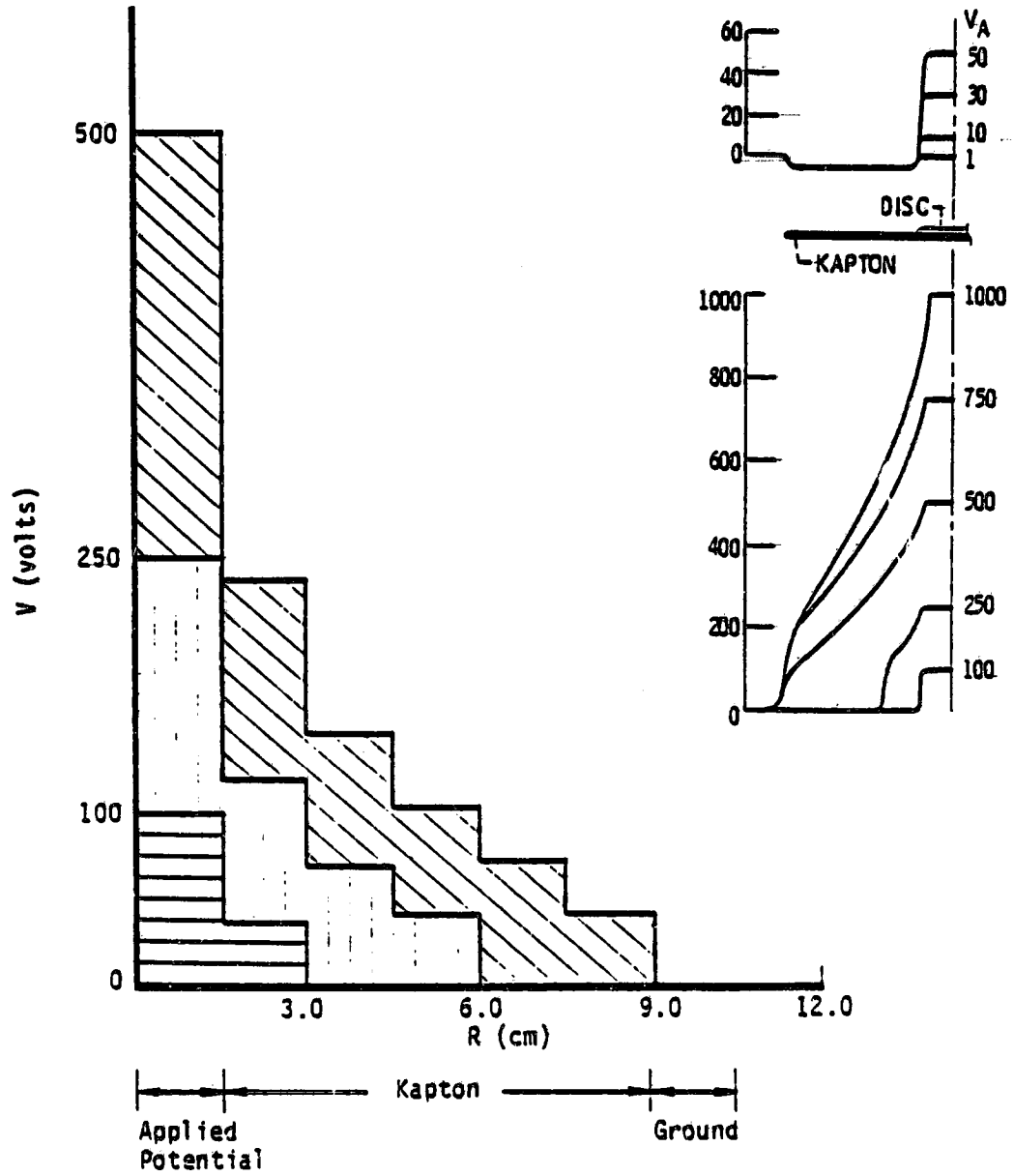

Figure 9. For high bias, NASCAP/LEO is in good agreement with experiment (inset) concerning the spread of high voltage onto the insulator.

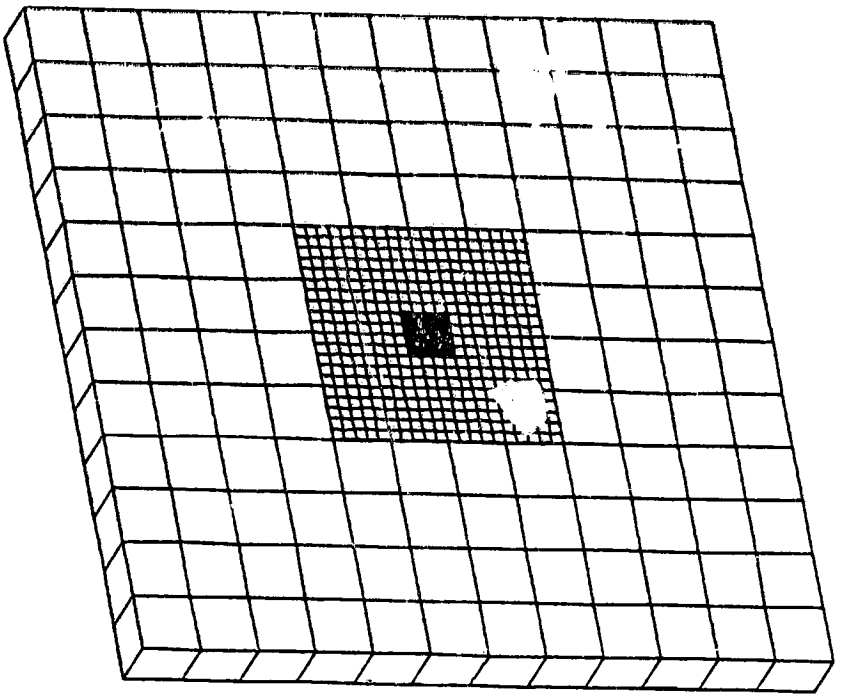

Figure 10. NASCAP model of biased pinhole experiment, showing sub-grid resolution of insulator surrounding 1.27 cm pinhole (central black area). The major grid resolution is 1.46 cm, and the subdivided region resolution is 0.29 cm.

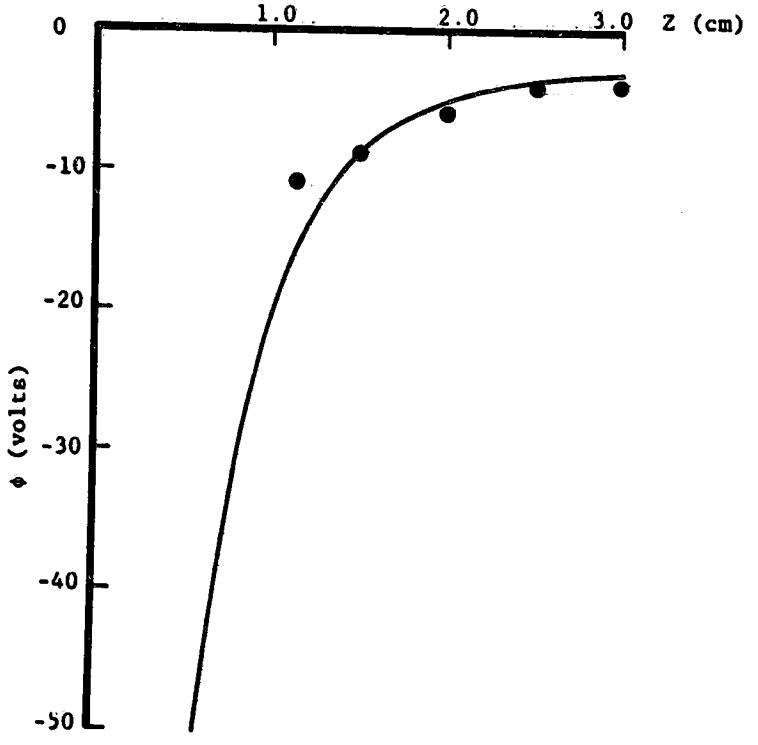

Figure 11. Potentials on axis for 0.64 cm diameter pinhole at -452 V. Solid line: Calculated with kapton at 0 volts; Points: Experiment.

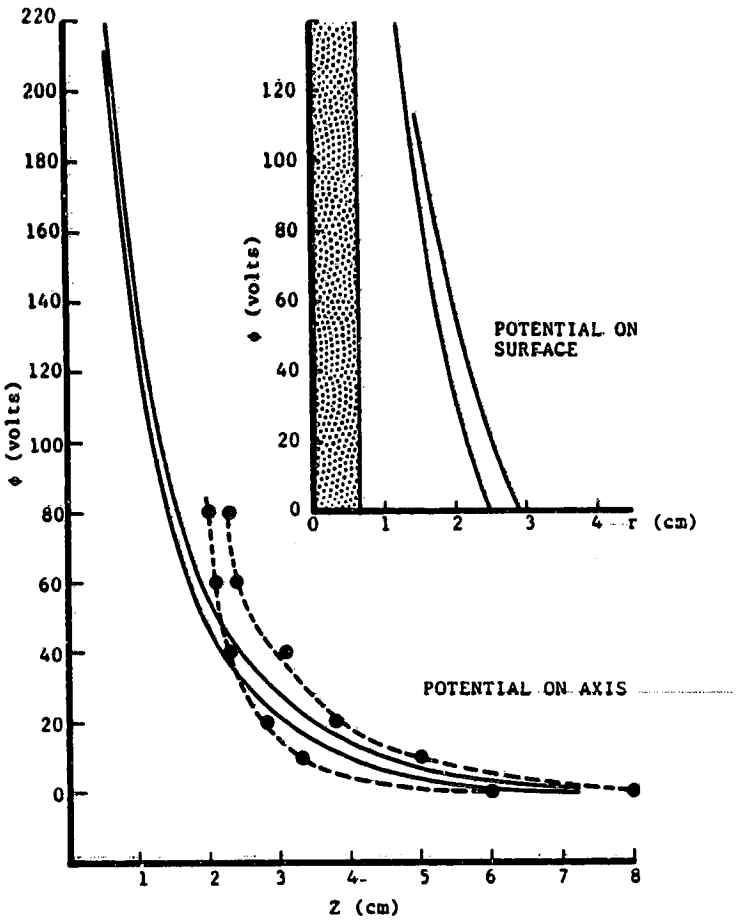

Figure 12. Potentials for 1.27 cm diameter pinhole.
Solid curves: Calculation.
Dashed curves: Experiment.
Upper curves: $n_e = 2.5 \times 10^4$ cm^{-3}, $\theta = 5.3$ eV.
Lower curves: $n_e = 5.8 \times 10^4$ cm^{-3}, $\theta = 4.0$ eV.

subdivision capability, and validated our electric field boundary condition model for the secondary electron layer.

FUTURE DEVELOPMENT

We plan to develop NASCAP/LEO for use as a reliable design tool. Among the planned improvements are prediction of spacecraft floating potential, treatment of sheath ionization, improved ram-wake model, generalization to full NASCAP geometry, and self-consistent power system representation. Validation/improvement cycles will continue at each stage, aided by both ground-based and space-based experiments.

REFERENCES

1. Katz, I.; Mandell, M. J.; Schnuelle, G. W.; Parks, D. E.; and Steen, P. G.: Plasma Collection by High-Voltage Spacecraft at Low Earth Orbit. J. Spacecraft and Rockets, 18, 1981, p. 79.

2. Mandell, M.J.; Katz, I.; and Cooke, D. L.: Potentials on Large Spacecraft in LEO. IEEE Transactions on Nuclear Science, NS-29, December 1982, pp. 1584-1586.

3. McCoy, J. E.; and Konradi, A.: Sheath Effects Observed on a 10 meter High Voltage Panel in Simulated Low Earth Orbit Plasma. Spacecraft Charging Technology-1978, NASA CP-2071, AFGL-TR-79-0082, 1978.

4. Cooke, D. L.; Parker, L. W.; and McCoy, J. E.: Three-Dimensional Space Charge Model for Large High-Voltage Satellites. Spacecraft Charging Technology-1980, NASA CP-2181, AFGL-TR-81-0270, 1981.

5. Grier, N. T.: Plasma Interaction Experiment II: Laboratory and Flight Results. Spacecraft Environment Interactions Technology Conference, Colorado Springs, CO, October 4-6, 1983.

6. Miller, W. L.: An Investigation of Arc Discharging on Negatively-Biased Dielectric-Conductor Samples in a Plasma. Spacecraft Environment Interactions Technology Conference, Colorado Springs, CO, October 4-6, 1983.

7. Snyder, D.: The Time Dependence of Discharges from a Biased Solar Array. Spacecraft Environment Interactions Technology Conference, Colorado Springs, CO, October 4-6, 1983.

8. Domitz, S.; and Kolecki, J. C.: Effect of Parasitic Plasma Currents on Solar Array Power Output. Spacecraft Charging Technology-1978, NASA CP-2071, AFGL-TR-79-0082, 1979.

9. Katz, I.; Cassidy, J. C.; Mandell, M. J.; Schnuelle, G. W.; Steen, P. G.; and Roche, J. C.: The Capabilities of the NASA Charging Analyzer Program. Spacecraft Charging Technology-1978, NASA CP-2071, AFGL-TR-79-0082, 1979.

10. Mandell, M. J.; Katz, I.; and Schnuelle, G. W.: Photoelectron Charge Density and Transport Near Differentially Charged Spacecraft. IEEE Transactions on Nuclear Science, NS-26, 1979, p. 5107.

11. Pelizzari, M. A.; and Criswell, D. R.: Differential Photoelectric Charging of Nonconducting Surfaces in Space. Journal of Geophysical Research, 83, 1978, p. 5233.

12. Mandell, M. J.; Katz, I.: Potentials in a Plasma Over a Biased Pinhole. Presented at 1983 IEEE 20th Annual Conference on Nuclear and Space Radiation Effects, Gatlinburg, TN, July 18-21, 1983; to be published in IEEE Transactions on Nuclear Science, NS-30, December 1983.

13. Stevens, N. J.; Berkopec, F. D.; Purvis, C. K.; Grier, N.; and Staskus, J.: Investigation of High Voltage Spacecraft System Interactions with Plasma Environments. AIAA/DGLR Electric Propulsion Conference, AIAA Paper No. 78-672, 1978.

14. Chaky, R. C.; Nonnast, J. H.; and Enoch, J.: A Numerical Simulation of Plasma-Insulator Interactions in the Spacecraft Environment. Journal of Applied Physics, 52, 1981, p. 7092.

15. Gabriel, S. B.; Garner, C. E.; and Kitamura, S.: Experimental Measurements of the Plasma Sheath Around Pinhole Defects in a Simulated High-Voltage Solar Array. AIAA Paper No. 83-0311, AIAA 21st Aerospace Sciences Meeting, Reno, NV, January 10-13, 1983.